Carbohydrate Polymers 89 (2012) 687–693

Contents lists available at SciVerse ScienceDirect

Carbohydrate Polymers

journal homepage: www.elsevier.com/locate/carbpol

Nanocomposites based on plasticized starch and rectorite clay: Structure and properties

Peter R. Chang [b,*], Dongliang Wu [a], Debbie P. Anderson [b], Xiaofei Ma [a,**]

[a] Chemistry Department, School of Science, Tianjin University, Tianjin 300072, China
[b] Bioproducts and Bioprocesses National Science Program, Agriculture and Agri-Food Canada, 107 Science Place, Saskatoon, SK, S7N 0X2, Canada

ARTICLE INFO

Article history:
Received 18 February 2012
Received in revised form 17 March 2012
Accepted 25 March 2012
Available online 3 April 2012

Keywords:
Composites
Plasticized starch
Rectorite
Cationic guar gum

ABSTRACT

Sodium rectorite clay (REC) was attached to cationic guar gum (CGG) using a cationic-exchange reaction to obtain CGG modified-REC (CREC). It was found that CGG appeared on the surface of REC's layered structure and represented about 30.1% wt. in CREC. REC and CREC were, respectively, used as fillers in a plasticized starch (PS) matrix to prepare PS/REC and PS/CREC composites using the casting process. Rapid Visco Analyser and scanning electron microscopy revealed that an interaction existed between the REC (or CREC) filler and the matrix. Both REC and CREC had obvious reinforcing effects on the matrix. Compared to the neat matrix, REC or CREC improved the thermal stability of the composites. By increasing the filler content from 0 to 10 wt%, water vapor permeability (WVP) values of PS/REC composites obviously decreased, while WVP values of PS/CREC composites decreased slightly.

1. Introduction

Public concern over the environment, climate change, and the depletion of fossil fuels has prompted many researchers to develop starch-based biocomposites or thermoplastics by exploiting the unique attributes of starch, i.e., biodegradability, renewability and low cost (Ma, Yu, & Wan, 2006; Shogren, Swanson, & Thompson, 1992; Van Soest & Knooren, 1997). However, their mechanical properties have disappointingly lagged behind their conventional petroleum-based counterparts.

The nano-sized fillers from natural clay minerals are often incorporated into plasticized starch (PS) matrices to improve the properties, due to their easy availability, versatility, and low environmental and health concerns. Unmodified montmorillonite (MMT) and organically modified MMT with different ammonium cations were, respectively, incorporated to prepare PS/MMT composites by melt processing (Park et al., 2002). Hectorite, kaolinite, and MMT have also been individually added to PS to obtain composites with improved properties (Chen & Evans, 2005). In addition, halloysite (HNT), a natural aluminosilicate nanotube, has been reported to enhance the pasting viscosity, tensile strength and thermal stability of PS/HNT composites (Xie, Chang, Wang, Yu, & Ma, 2011). Similarly, needle-shaped natural sepiolite and cationic starch modified sepiolite have been incorporated into PS (Chivrac, Pollet, Schmutz, & Avérous, 2010). It is worth mentioning that improvements in properties depend greatly on the interactions between the matrix and the clay fillers. Interestingly, when these fillers were introduced, the tensile strength of the composites increased without decreasing the elongation at break.

Rectorite (REC) is a type of regularly interstratified clay mineral with alternating pairs of a dioctahedral mica-like layer and a dioctahedral smectite-like layer. The interlayer cations of REC can be easily exchanged with either organic or inorganic cations (Wu, Zheng, Chang, & Ma, 2011). Research on organically modified rectorite (OREC) composites based on polyurethane elastomer, polypropylene, natural rubber, and chitosan has been carried out, and results show that the addition of OREC can confer polymers higher mechanical and thermal properties (Yang, Liang, Zhang, He, & Wang, 2009). However, the introduction of REC into PS has not been reported before. In this work, REC was firstly treated with cationic guar gum (CGG) by a cationic-exchange reaction to obtain CGG modified-REC (CREC), which added polysaccharide components onto REC. This work focuses on processing and characterization of PS/REC and PS/CREC composites in terms of morphology, thermogravimetric analysis, pasting viscosity, mechanical properties and water vapor permeability.

2. Experimental

2.1. Materials

Potato starch was supplied by Manitoba Starch Products (Manitoba, Canada). Sodium rectorite (REC) was obtained from Hubei

* Corresponding author.
** Corresponding author. Tel.: +86 22 27406144; fax: +86 22 27403475.
E-mail addresses: peter.chang@agr.gc.ca (P.R. Chang), maxiaofei@tju.edu.cn (X. Ma).

0144-8617/$ – see front matter.
http://dx.doi.org/10.1016/j.carbpol.2012.03.076

Zhongxiang Rectorite Mine (Wuhan, China). Cationic guar gum (CGG) JK140 (with quaternary ammonium cationic functions) was provided by Jingkun Chemistry Company, Jiangsu, China. All other reagents were of analytical grade purchased from Tianjin Chemical Reagent Factory (Tianjin, China).

2.2. Preparation of PS/REC composites

REC was dispersed into a solution of distilled water (100 mL) and glycerol (1.5 g) using ultrasonication for 10 min. Starch, 5 g in quantity, was subsequently added. The REC loading level (0, 2, 4, 6, 8 or 10 wt%) was based on starch. The mixture was heated at 90 °C for 0.5 h with constant stirring to plasticize the starch. The mixture was then cast into a film on a dish and placed in an air-circulating oven at 50 °C until dry (about 6 h). The PS/REC composite films were preconditioned in a climate chamber at 25 °C and 50% RH for at least 48 h prior to testing.

2.3. Preparation of PS/CREC composites

REC was dispersed into a solution of distilled water (50 mL) using ultrasonication for 10 min. A quantity of 0.5 g of CGG was completely dissolved in 70 mL of distilled water (pH = 5–6). A mixture of the two solutions was reacted at 60 °C for 4 h, and CGG-modified REC (CREC) was thereby formed in the solution. The REC loading level (0, 2, 4, 6, 8 or 10 wt%) was based on starch. Glycerol (1.5 g), starch (5 g) and distilled water (30 mL) were added into the obtained CREC solution and the mixture heated at 90 °C for 0.5 h with constant stirring for the plasticization of starch. The mixture was cast into a film and dried in an air-circulating oven at 50 °C. The PS/CREC composite films about 0.2 mm thick were preconditioned in a climate chamber at 25 °C and 50% RH for at least 48 h prior to testing.

A CREC powder was prepared for characterization. REC (2 g) was added into 200 mL of distilled water and dispersed in an ultrasonic bath at room temperature for 10 min. CGG (2 g) was dissolved into 280 mL of distilled water (pH = 5–6). A mixture of these solutions was reacted at 60 °C for 4 h. The solution was centrifuged and washed with distilled water. The obtained CREC were washed by ethanol, and dried at 50 °C for 12 h.

2.4. Fourier transform infrared spectroscopy (FTIR)

FTIR analysis of REC, CGG and CREC was performed on a BIO-RAD FTS3000 IR Spectrum Scanner. The sample powders were evenly dispersed in KBr and pressed into transparent sheets for testing.

2.5. Transmission electron microscopy (TEM)

A suspension of CREC was dropped onto a copper grid which was coated with a carbon film, air-dried, and then examined using a Tecnai G2 F20 TEM.

2.6. Thermogravimetric (TG) analysis

Thermal properties of REC, CGG and CREC and the composites were measured with a STA 409 PC thermal analyzer, NETZSCH, Germany. The weights of the samples were about 10–15 mg, and they were heated from room temperature to 600 °C at a heating rate of 15 °C/min in a nitrogen atmosphere.

2.7. Scanning electron microscopy (SEM)

The fracture surfaces of PS/CREC and PS/REC composites were viewed with a NanoSEM 430 scanning electron microscope. The composites were cooled in liquid nitrogen, and then broken. The fracture faces were vacuum coated with gold for SEM.

2.8. Rapid visco analyser (RVA)

To ensure that the cold slurries used for RVA had the same composition as the mixtures used for casting the PS/REC composites, RECs (0, 0.02, 0.04, 0.06, 0.08 and 0.1 g) were, respectively, dispersed into solutions of distilled water (20 mL) and glycerol (0.3 g) using ultrasonication for 10 min before 1 g starch was added. Similarly, cold slurries of PS/CERC were prepared at one-fifth scale of that in Section 2.3 but without heating to 90 °C for 0.5 h. The obtained cold slurries of PS/REC and PS/CREC were then subjected to a heating/holding/cooling protocol using a Rapid Visco Analyser (Newport Scientific, Sydney, Australia) according to AACC method 76-21 (Ma, Chang, Yang, & Yu, 2009). Specifically, the RVA profile used kept the starch containing slurry at 50 °C for 1 min, then heated to 95 °C at 12.2 °C/min and held at 95 °C for 2.5 min. It was then cooled to 50 °C (cooling rate of 11.8 °C/min) and kept at 50 °C for 2 min. The paddle speed was 960 rpm for 10 s and then decreased to 160 rpm for the rest of the experiment.

2.9. Mechanical testing

A Testometric AX M350-10KN materials testing machine was operated at a crosshead speed of 50 mm/min for tensile testing (ISO 1184-1983 standard). Samples were conditioned at 25 °C and 50% RH for 48 h before testing. The data were averaged over 6–8 specimens.

2.10. Water vapor permeability (WVP)

WVP tests were carried out using ASTM method E96 (1996) with some modifications (Yu, Yang, Liu, & Ma, 2009). The films were cut into circles, sealed over with melted paraffin, and stored in a desiccator at 25 °C. RH 0% was maintained using anhydrous calcium chloride in the cell. Each cell was placed in a desiccator containing saturated sodium chloride to provide a constant RH 75%. Water vapor transport was determined by the weight gain of the permeation cell. Slopes were calculated by linear regression (weight change vs. time). The water vapor transmission rate (WVTR) was defined as the slope (g/s) divided by the transfer area (m^2). After the permeation tests, film thickness was measured and WVP ($gm^{-1}\ s^{-1}\ Pa^{-1}$) was calculated as

$$\mathrm{WVP} = \frac{\mathrm{WVTR}}{P(R_1 - R_2)} \cdot x$$

where P is the saturation vapor pressure of water (Pa) at the test temperature (25 °C), R_1 is the RH in the desiccator, R_2, the RH in the permeation cell and x is the film thickness (m). Under these conditions, the driving force $[P(R_1 - R_2)]$ is 1753.55 Pa.

3. Results and discussion

3.1. Characterization of CREC

As shown in Fig. 1(a), neat REC exhibited platelets with a lateral size of about 1 μm and a thickness of about 50–100 nm, while REC attached/associated to CGG in CREC (in Fig. 1b). It implied the high affinity between CGG and REC. Since the interlayer cations of REC can be easily exchanged with either organic or inorganic cations (Yang et al., 2009), the quaternary ammonium of CGG attached to the layered REC structure to form CREC by cationic-exchange. However, REC layers were not exfoliated, because the platelets did not obviously become smaller.

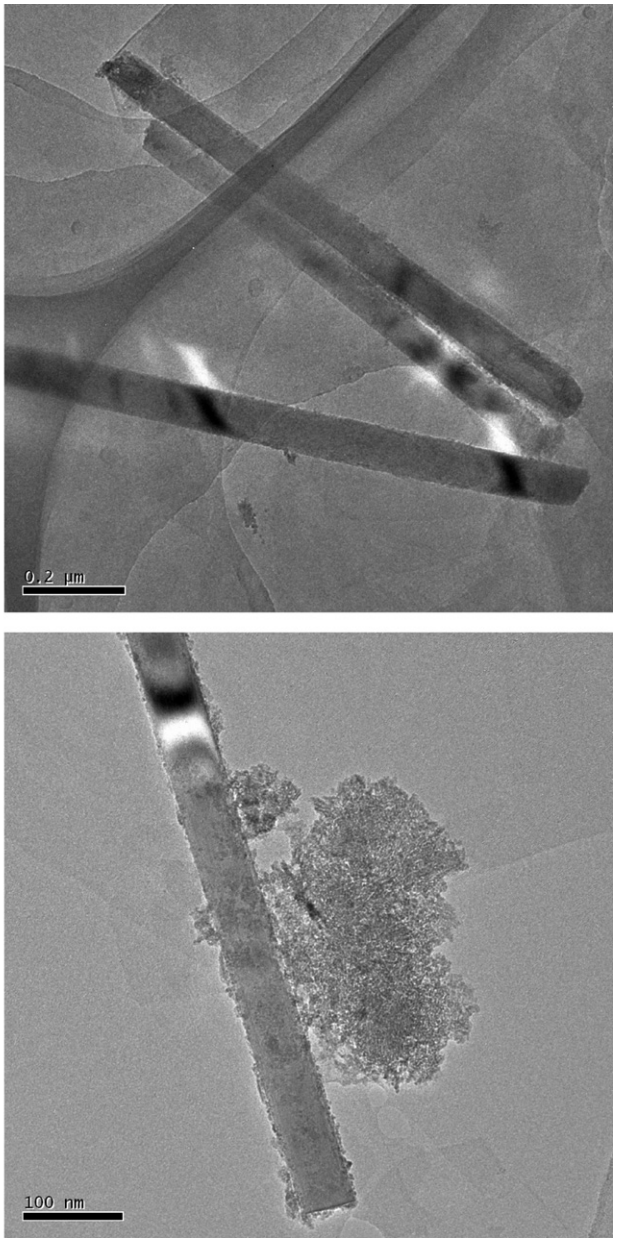

Fig. 1. TEM of REC (a) and CREC (b).

Fig. 2 shows the FTIR spectra of CGG, REC and CREC. The peaks at 3440 and 3644 cm^{-1} were attributed to the bending vibration of the hydrogen band of interlaminar water and the hydroxyl stretching of SiOH (Yang et al., 2009). And the hydroxyl bending of water appeared at 1640 cm^{-1} (Wang et al., 2010). The peaks at 1050 cm^{-1} were associated with the Si–O stretching vibration, while the peaks at 460–540 cm^{-1} were assigned to the Si–O bending vibration. As shown in the FTIR spectrum of CGG, the absorption band at about 2920 cm^{-1} was attributed to CH_2 stretching vibration of CGG, while the bonds at 900–1200 cm^{-1} were the fingerprint region of the –C–O–C– stretching vibration in the anhydroglucose ring. The spectrum of CREC was quite similar to REC except for the CH_2 stretching vibration of CGG at 2920 cm^{-1}. The Si–O band of REC at 1050 cm^{-1} and the –C–O–C– stretching vibration of CGG at 900–1200 cm^{-1} could overlap those in CREC. Since REC has an ion exchange capacity, the cationic quaternary ammonium of CGG could be adsorbed onto the REC; thereby CGG attached to REC and formed an interaction with REC in CREC.

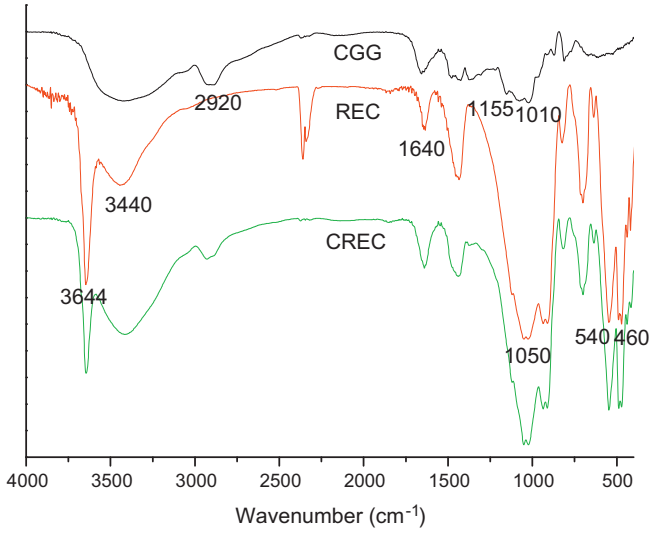

Fig. 2. FTIR spectra of CGG, REC and CREC.

The thermogravimetric (TG) and derivative thermogravimetric (DTG) curves of REC, CGG and CREC are shown in Fig. 3. The thermal decomposition temperature appeared at the maximum rate of mass loss, i.e. the peak temperature shown in DTG curves. REC did not decompose below 550 °C. The decomposition temperature of CGG was 280 °C, while that of CGG in CREC was 286 °C. CGG exhibited lower thermal stability than CGG in CREC, which could be ascribed to the interaction between REC and CGG. The CREC showed a weight loss of about 16.7 wt% at the thermal decomposition temperature of CGG. The quantity of CGG was calculated by matching the percentage weight loss of CREC to the percentage weight loss of CGG at the decomposition temperature (about 55.5 wt%). The CGG content of CREC was estimated to be about 30.1 wt%.

3.2. SEM of composites

Native cornstarch exists in the form of granules. However, when the continuous phase of the matrix for the composites formed, no residual granules appeared, as shown in Fig. 4(a) and (b), although CGG agglomeration was observed in the matrix, as revealed in Fig. 4(b). Both REC and CREC (Fig. 4c and d) dispersed well in the matrix at low loading levels (2 wt%), but agglomeration of CREC was

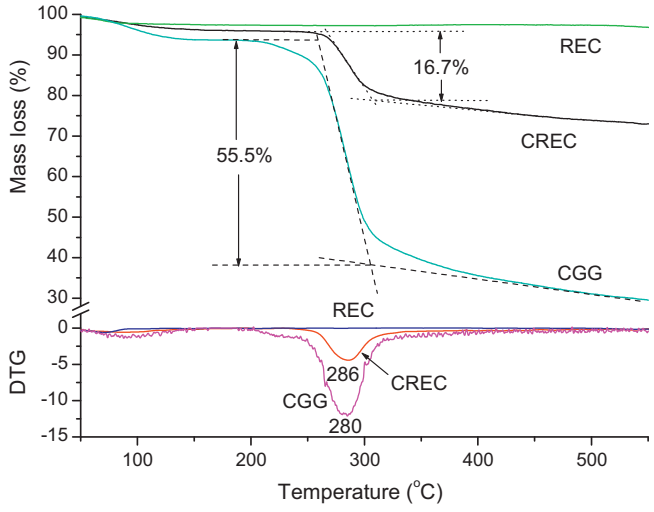

Fig. 3. Thermogravimetric (TG) and derivative thermogravimetric (DTG) curves of CGG, REC and CREC.

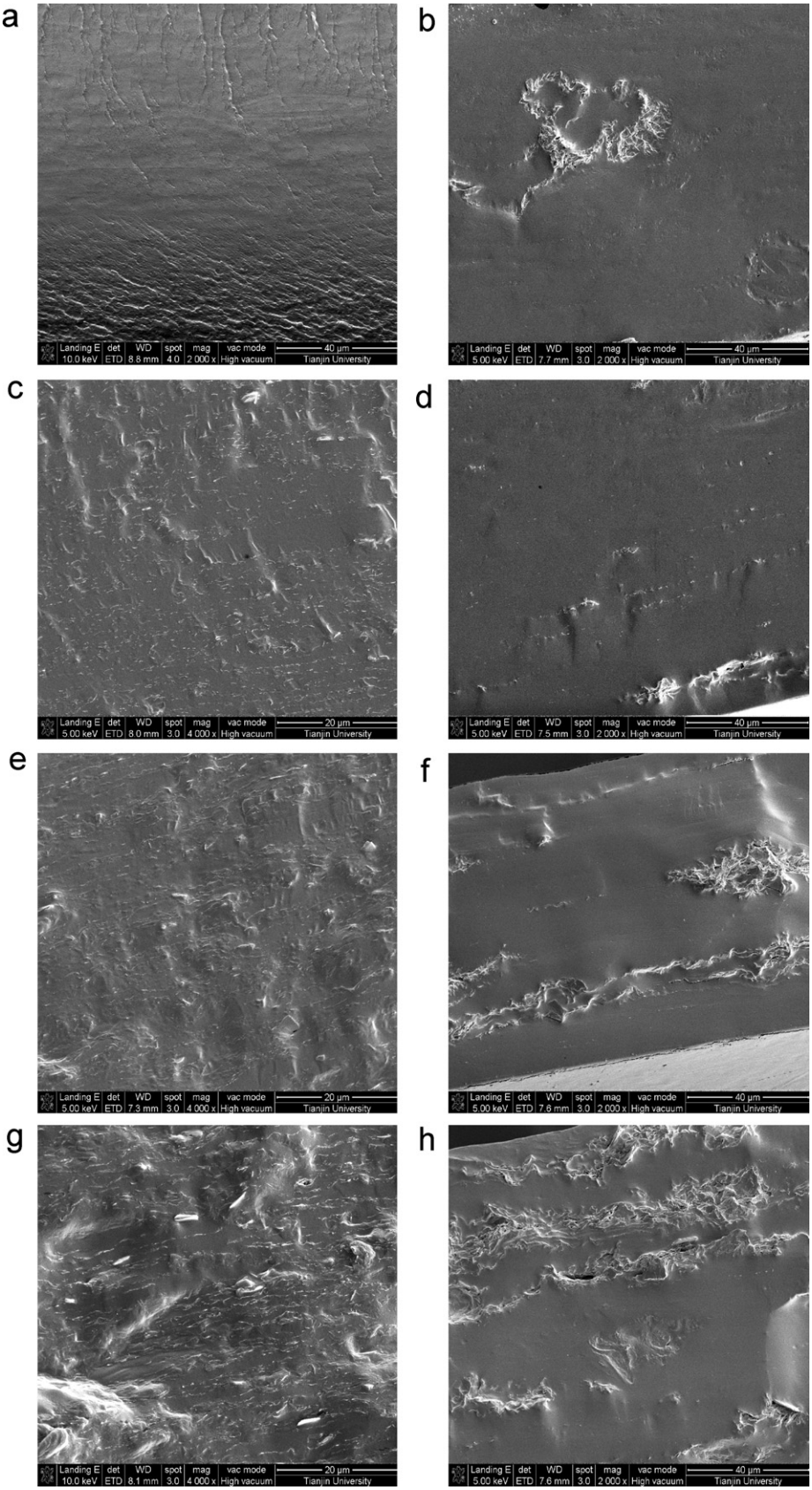

Fig. 4. SEM micrograph of the fragile fractured surfaces of PS/REC (a, c, e and g) and PS/CREC (b, d, f and h) composites. The filler contents: 0 wt% (a, b), 2 wt% (c, d), 6 wt% (e, f) and 10 wt% (g, h).

also observed. When the REC and CREC contents were increased (Fig. 4e–h), REC exhibited good dispersion in the matrix even at 10 wt%, while more and more agglomeration of CREC was noticeably visible. It was disappointing to learn that CREC had poor dispersion as compared to REC. This may be related to the CGG components aggregating at low water levels while the solution dried in the casting process. Therefore, CREC agglomerated more in PS/CREC composites than REC in PS/REC composites. In addition, the surfaces of REC or CREC agglomerations appeared to be covered by the matrix, which was related to strong interactions. SiOH groups in REC could form hydrogen bond interactions with starch in PS/REC composites (Wang et al., 2010), while CGG in CREC formed interactions with starch because of their similar polysaccharide structures.

3.3. RVA

The effects of REC concentration on the viscosity of PS/REC and PS/CREC casting solutions were studied by the Rapid Visco Analyser using a heating–cooling program, as described in Section 2.8. In order to simulate the processing of composites, a slurry identical to the casting solution was used in RVA analysis. As listed in Table 1, the REC concentration had little effect on the pasting temperature of starch. Because the water contents of the PS/REC and PS/CREC casting solutions were different, their pasting viscosities were different even when the REC contents were the same. The relative values of the viscosity, based on the viscosity of the matrix, are listed in brackets to estimate the effect of REC on the pasting viscosities of PS/REC and PS/CREC casting solutions. For both PS/REC and PS/CREC casting solutions, the higher the REC content was, the higher the viscosities of casting solutions were. When 0.1 g REC was added, i.e., REC was below 0.5 wt% of casting solutions, the peak viscosity, holding strength, and final viscosity increased 31%, 19% and 19%, respectively, for PS/REC casting solutions. For PS/CREC casting solutions, these numbers increased 38%, 28% and 24%, respectively. This showed that CREC formed stronger interactions with starch than REC did.

3.4. Mechanical properties of composites

Fig. 5 shows the effect of filler content on the mechanical properties of PS/REC and PS/CREC composites. As the filler, REC had an obvious reinforcing effect on the matrix of PS/REC and PS/CREC composites. The tensile strength of the PS matrix and PS/CGG matrix without REC were 4.7 and 6.5 MPa, respectively. When only 2 wt% REC was added, the tensile strengths of PS/REC and PS/CREC composites reached 18.3 and 17.8 MPa, respectively. With increasing filler content, the tensile strength gradually decreased to 13.2 and 11.2 MPa, respectively, at the loading level of 10 wt% filler. This obvious reinforcing effect at low REC content was ascribed to good interfacial interaction between the filler and matrix. At greater than 2 wt% of REC, the tensile strength of the composites decreased, which may be ascribed to agglomeration of the fillers. Interestingly, the tensile strength of PS/CREC was lower than that of PS/REC, primarily due to the fact that agglomeration of CREC was more severe than REC in their respective composites. Agglomeration in CREC or REC indeed decreased the effectiveness of these reinforcement fillers. These results were consistent with the results of SEM.

When the filler content was varied from 0 to 10 wt%, the elongation at break decreased from 40.7% to 28.7% for PS/REC composites and from 48% to 27.1% for PS/CREC composites. The fillers may constrain the surrounding polymers, decrease the mobility of matrix chains, and result in lower elongation at break.

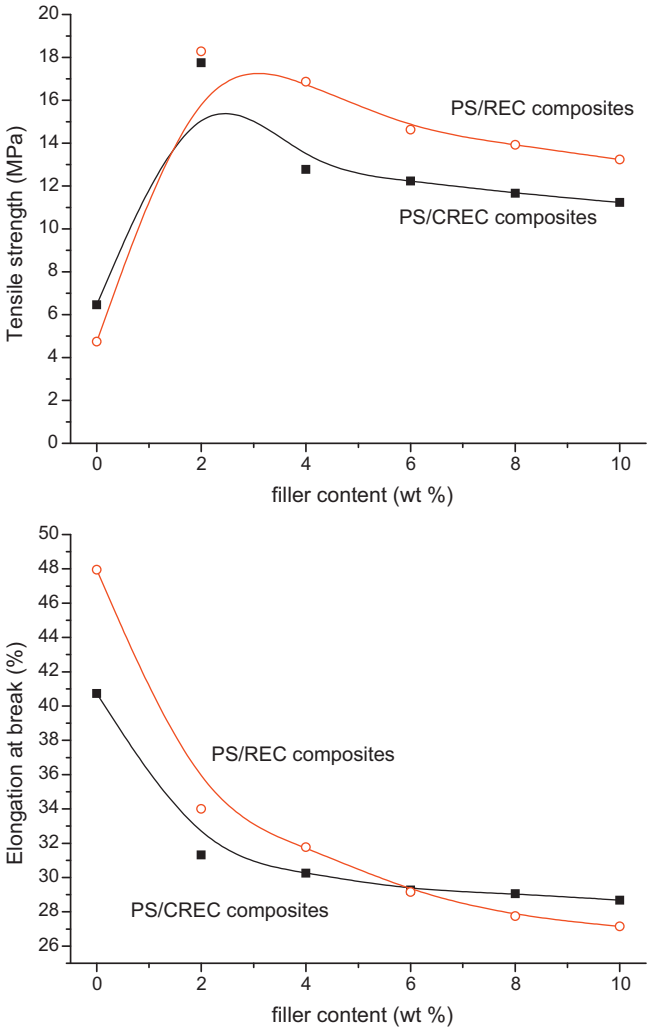

Fig. 5. The effect of filler content on tensile yield strength and elongation at break of PS/REC and PS/CREC composites.

3.5. Thermal stability of composites

TG and DTG curves of PS/REC and PS/CREC composites are shown in Fig. 6. The degradation of PS took place at 315 °C, while PS/REC composites containing 2 wt% REC degraded at 327 °C. The addition of REC increased the thermal stability of PS; however, when more REC (6 and 10 wt%) was added, the thermal stability of the PS/REC composites deceased slightly. This could be ascribed to agglomeration of REC. Similarly, PS/REC composites with 2 wt% REC exhibited the maximal tensile strength.

The matrix of PS/CREC composites exhibited two peaks in the DTG curve, which were attributed to the decompositions of CGG and PS at 270 °C and 300 °C, respectively. Both were lower than pure CGG (280 °C) and pure PS (315 °C). Water and (or) glycerol may accelerate the decomposition of CGG, which decreased the decomposition temperature of PS. When filler (2 wt%) was added to PS/CREC composites, the decomposition temperatures of CGG and PS appeared higher, at 283 °C and 300 °C, respectively. And higher filler contents (6 and 10 wt%) further improved the thermal stability of PS/CREC composites. Although CREC agglomerated, the stronger interaction between CREC and PS made the decomposition of composites occur at a higher temperature than composites made with REC and PS.

Table 1
The effect of filler content on the processing characteristics of PS/REC and PS/CREC casting solutions.

Filler content (%)	Pasting temperature (°C)	Peak viscosity (cp)	Holding strength (cp)	Final viscosity (cp)
PS/REC composites				
0	70.0	1503 (1.00)	1081 (1.00)	1332 (1.00)
2	70.0	1543 (1.03)	1112 (1.03)	1463 (1.11)
4	70.1	1659 (1.10)	1197 (1.11)	1491 (1.12)
6	70.0	1777 (1.18)	1223 (1.13)	1511 (1.13)
8	70.1	1886 (1.25)	1258 (1.16)	1543 (1.16)
10	70.2	1975 (1.31)	1283 (1.19)	1582 (1.19)
PS/CREC composites				
0	76.8	497 (1.00)	386 (1.00)	493 (1.00)
2	77.6	528 (1.06)	411 (1.06)	503 (1.02)
4	77.7	543 (1.09)	432 (1.12)	531 (1.08)
6	77.8	585 (1.18)	457 (1.18)	553 (1.12)
8	77.5	628 (1.26)	486 (1.26)	587 (1.19)
10	77.8	686 (1.38)	493 (1.28)	612 (1.24)

The data in brackets are relative values of the viscosity characteristics related to the matrix viscosity characteristics.

3.6. WVP of composites

Water vapor permeability (WVP) was used to study moisture transport through the PS/REC and PS/CREC composite films. As shown in Fig. 7, water vapor easily permeated the PS film with the highest WVP values of 9.88×10^{-10} gm^{-1} s^{-1} Pa^{-1}. The introduction of CGG decreased the WVP value of the matrix for the PS/CREC composite. With the increasing of filler content from 0 to 10 wt%, WVP values of PS/REC decreased obviously, from 9.88 to 2.61×10^{-10} gm^{-1} s^{-1} Pa^{-1}, while WVP values of PS/CREC decreased from 7.14 to 4.11×10^{-10} gm^{-1} s^{-1} Pa^{-1}. When the filler content was greater than 2 wt%, WVP values for PS/REC composites were lower than those for PS/CREC composites. The addition of the filler probably introduced a tortuous path for water molecules to pass through the composite films (Chang, Jian, Zheng, Yu, & Ma, 2010). When the filler content was increased, the aggregation of CREC in the matrix was more obvious. The PS/REC composites exhibited a better water vapor barrier in comparison with PS/CREC composites.

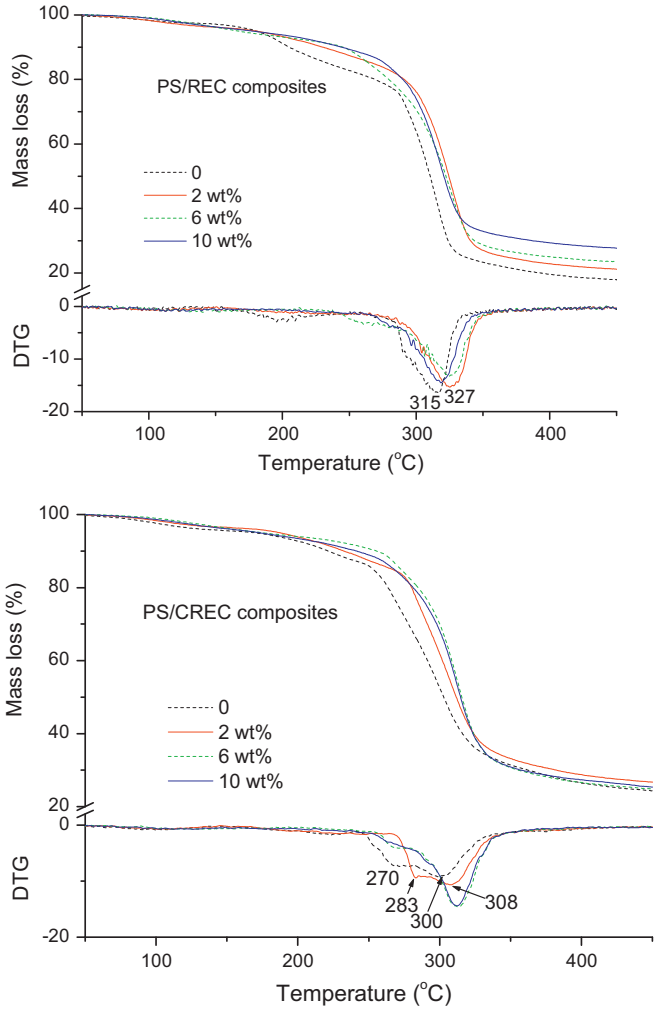

Fig. 6. The effect of filler content on thermal stability of PS/REC and PS/CREC composites.

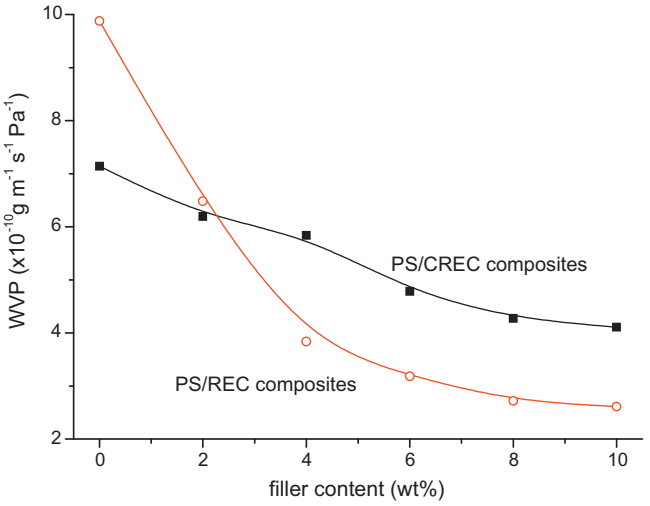

Fig. 7. The effect of filler content on water vapor permeability of PS/REC and PS/CREC composites.

4. Conclusions

In the present study, CREC was prepared by modifying REC with CGG using a cationic-exchange reaction. With increasing filler content, the viscosities of PS/REC and PS/CREC casting solutions increased, as a result of interactions between REC (or CREC) and gelatinized starch. Since the relative viscosity values were higher for PS/CREC than PS/REC casting solutions, CREC may form a stronger interaction with starch than REC. The introduction of REC and CREC improved the tensile strength, thermal stability, and water vapor barrier of the composites in comparison with the pure matrix. Because CREC filler agglomerated more in PS/CREC composites than REC filler did in PS/REC composites, the tensile strength

and water vapor barrier of PS/REC composites were higher than those of PS/CREC composites.

The PS/CREC and PS/REC composites will have potential applications in food and one-off packaging. In addition, REC and CREC could also be used as filler in natural polysaccharide (guar gum, agar, alginate and chitosan) matrices.

References

Chang, P. R., Jian, R. J., Zheng, P. W., Yu, J. G., & Ma, X. F. (2010). Preparation and properties of glycerol plasticized-starch (GPS)/cellulose nanoparticle (CN) composites. *Carbohydrate Polymers*, *79*, 301–305.

Chen, B. Q., & Evans, J. R. G. (2005). Thermoplastic starch-clay nanocomposites and their characteristics. *Carbohydrate Polymers*, *61*, 455–463.

Chivrac, F., Pollet, E., Schmutz, M., & Avérous, L. (2010). Starch nano-biocomposites based on needle-like sepiolite clays. *Carbohydrate Polymers*, *80*, 145–153.

Ma, X. F., Chang, P. R., Yang, J. W., & Yu, J. G. (2009). Preparation and properties of glycerol plasticized-pea starch/zinc oxide-starch bionanocomposites. *Carbohydrate Polymers*, *75*, 472–478.

Ma, X. F., Yu, J. G., & Wan, J. J. (2006). Urea and ethanolamine as a mixed plasticizer for thermoplastic starch. *Carbohydrate Polymers*, *64*, 267–273.

Park, H. M., Li, X. C., Jin, C. Z., Park, C. Y., Cho, W. J., & Ha, C. S. (2002). Preparation and properties of biodegradable thermoplastic starch/clay hybrids. *Macromolecular Materials and Engineering*, *287*, 553–558.

Shogren, R. L., Swanson, C. L., & Thompson, A. R. (1992). Extrudates of cornstarch with urea and glycols: Structure/mechanical property relations. *Starch/Stärke*, *44*, 335–338.

Van Soest, J. J. G., & Knooren, N. (1997). Influence of glycerol and water content on the structure and properties of extruded starch plastic sheets during aging. *Journal of Applied Polymer Science*, *64*, 1411–1422.

Wang, X. Y., Liu, B., Ren, J. L., Liu, C. F., Wang, X. H., Wu, J., et al. (2010). Preparation and characterization of new quaternized carboxymethyl chitosan/rectorite nanocomposite. *Composites Science and Technology*, *70*, 1161–1167.

Wu, D. L., Zheng, P. W., Chang, P. R., & Ma, X. F. (2011). Preparation and characterization of magnetic rectorite/iron oxide nanocomposites and its application for the removal of the dyes. *Chemical Engineering Journal*, *174*, 489–494.

Xie, Y. F., Chang, P. R., Wang, S. J., Yu, J. G., & Ma, X. F. (2011). Preparation and properties of halloysite nanotubes/plasticized *Dioscorea opposita* Thunb starch composites. *Carbohydrate Polymers*, *83*, 186–191.

Yang, L. L., Liang, G. Z., Zhang, Z. P., He, S. B., & Wang, J. H. (2009). Sodium alginate/Na^+-rectorite composite films: Preparation, characterization and properties. *Journal of Applied Polymer Science*, *114*, 1235–1240.

Yu, J. G., Yang, J. W., Liu, B. X., & Ma, X. F. (2009). Preparation and characterization of glycerol plasticized-pea starch/ZnO-carboxymethylcellulose sodium nanocomposites. *Bioresource Technology*, *100*, 2832–2841.